Organic & Biomolecular Chemistry

ROYAL SOCIETY OF CHEMISTRY

COMMUNICATION

View Article Online
View Journal | View Issue

Cite this: *Org. Biomol. Chem.*, 2020, **18**, 5125

Received 24th May 2020,
Accepted 19th June 2020

DOI: 10.1039/d0ob01076f

rsc.li/obc

On the reciprocal relationship between σ-hole bonding and (anti)aromaticity gain in ketocyclopolyenes†

Hari Ram Paudel,‡ Lucas José Karas ‡ and Judy I-Chia Wu *

σ-Hole bonding interactions (*e.g.*, tetrel, pnictogen, chalcogen, and halogen bonding) can polarize π-electrons to enhance cyclic [4*n*] π-electron delocalization (*i.e.*, antiaromaticity gain) or cyclic [4*n* + 2] π-electron delocalization (*i.e.*, aromaticity gain). Examples based on the ketocyclopolyenes: cyclopentadienone, tropone, and planar cyclononatetraenone are presented. Recognizing this relationship has implications, for example, for tuning the electronic properties of fulvene-based π-conjugated systems such as 9-fluorenone.

This paper discusses the reciprocal relationship between σ-hole bonding and (anti)aromaticity in heterocycles. We recently reported that intermolecular hydrogen bonding interactions can be used to modulate aromaticity and antiaromaticity in π-conjugated ring compounds,[1,2] and now show, in light of the recognized similarity between hydrogen bonding and σ-hole bonding,[3] that interactions such as tetrel,[4–7] pnictogen,[8,9] chalcogen,[10–13] and halogen[14–17] bonding interactions also can perturb the (anti)aromatic characters of π-conjugated ring compounds such as cyclopentadienone, tropone, and planar cyclononatetraenone in the same way.

σ-Hole interactions like tetrel, pnictogen, chalcogen, and halogen bonding (Y···X–R) are highly directional noncovalent interactions that form between a negative site (Y, *e.g.*, a Lewis base or anion) and the electron-deficient region of a covalently-bonded group 14–17 atom (X).[18–21] The R group generally includes one or more electron-withdrawing groups, and a σ-hole forms due to an uneven distribution of atomic charge on X. σ-Hole interactions are predominantly electrostatic,[22,23] although the relevance of polarization, dispersion, and charge transfer effects have been recognized.[24–28] Strong tetrel, pnictogen, chalcogen, and halogen bonding interactions were found to display donor–acceptor orbitals interactions.[29] Heavier and more polarizable atoms can exhibit pronounced σ-holes and form very strong σ-hole interactions.

Even though tetrel, pnictogen, chalcogen, and halogen bonding arise as a result of a polarized σ-bond, these bonding interactions can indirectly polarize the π-system of an interacting Lewis base. For example, σ-hole bonding between the oxygen lone pair of a C=O Lewis base and an X–R group increases negative charge on the oxygen atom and enhances the resonance contribution of a polarized π-bond (*i.e.*, C^{+}–O^{-}), as shown by previous examples of C=O activation *via* σ-hole bonding.[30,31] In this paper, we relate the strengths of σ-hole interactions of C=O groups to the effects of (anti)aromaticity gain in ketocyclopolyene compounds, using the formally [4*n*] antiaromatic cyclopentadienone (four ring π-electrons), [4*n* + 2] aromatic tropone (six ring π-electrons), and [4*n*] antiaromatic planar cyclononatetraenone (eight ring π-electrons)[32–34] as models for the interacting Lewis base.

In cyclopentadienone, **1**, C^{+}–O^{-} polarization from σ-hole bonding enhances antiaromatic character of the five membered ring (*i.e.*, increased cyclic [4*n*] π-electron delocalization),[35] and the corresponding σ-hole bonding interaction is weakened (see Fig. 1a, resonance structure in green, resembling a cyclopentadienyl cation). In tropone, **2**, C^{+}–O^{-} polariz-

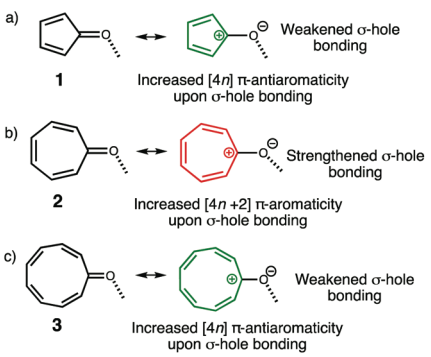

Fig. 1 Illustration of (anti)aromaticity gain on the strengths of σ-hole bonding in (a) cyclopentadienone, (b) tropone, and (c) cyclononatetraenone.

Department of Chemistry, University of Houston, Houston, TX 77204, USA.
E-mail: jiwu@central.uh.edu

†Electronic supplementary information (ESI) available: Planarization energies and Cartesian coordinates. See DOI: 10.1039/d0ob01076f

‡These authors contributed equally to this work.

ation from σ-hole bonding enhances aromatic character in the seven membered ring (*i.e.*, increased cyclic [4*n* + 2] π-electron delocalization),[33,36–38] and the corresponding σ-hole interaction is strengthened (see Fig. 1b, resonance structure in red, resembling a tropylium cation). In planar cyclononatetraenone, **3**, C^{+}–O^{-} polarization from σ-hole bonding enhances antiaromatic character in the nine membered ring (*i.e.*, increased cyclic [4*n*] π-electron delocalization),[33] and just as in **1**, the corresponding σ-hole interaction is weakened (see Fig. 1c, resonance structure in green). Fig. 1 illustrates the reciprocal relationships between σ-hole bonding and (anti)aromaticity gain in **1**, **2** and **3**.

We evaluated a series of tetrel, pnictogen, chalcogen, and halogen bonded complexes, in which *Y* = **1–3**, and X–R = GeH_3F (**a**), AsH_2F (**b**), SeHF (**c**), and BrF (**d**). Geometry optimization for all monomers, **1–3**, and complexes, **1(a–d)**, **2(a–d)**, and **3(a–d)** were performed at ωB97XD/def2-TZVP employing Gaussian16.[39] The choice of functional was selected based on benchmark studies of the XB18 and XB51 set using different DFT functionals.[40] Vibrational frequency analysis verified the nature of the stationary points. Cyclononatetraenone, **3**, has a non-planar minimum, but the symmetry constrained C_s form is used here to model a formally eight π-electron antiaromatic ring. Planar cyclononatetraenone, **3**, and complexes **3(a–d)** have imaginary frequencies corresponding to distortion of the nine membered ring from planarity (see details in the ESI†). Single point σ-hole interaction energies (ΔE_{int}) for the complexes, **1(a–d)**, **2(a–d)**, and **3(a–d)**, were carried out at MP2/def2-TZVP.

Electrostatic potentials *V*(r), calculated with a ρ(r) = 0.001 au (electrons $bohr^{-3}$)[41] contour at ωB97XD/def2-TZVP, identified the locations of the most positive electrostatic potentials ($V_{S,max}$) corresponding to the σ-holes of the X atoms of X–R: GeH_3F ($V_{S,max}$ = +40.6 kcal mol^{-1}), AsH_2F (+41.6 kcal mol^{-1}), SeHF (+46.9 kcal mol^{-1}), and BrF (+50.7 kcal mol^{-1}), following the order: halogen > chalcogen > pnictogen > tetrel (see Fig. 2, region colored in blue).

Computed interaction energies (ΔE_{int}) for halogen, chalcogen, pnictogen, and tetrel bonding interactions in **1(a–d)**, **2(a–d)**, and **3(a–d)** (see Table 1) follow the same order: halogen (σ-hole bonding to BrF) > chalcogen (σ-hole bonding to SeHF) > pnictogen (σ-hole bonding to AsH_2F) > tetrel (σ-hole bonding to GeH_3F) interactions, correlating to the magnitude of the positive electrostatic potentials of the σ-holes. Accordingly, computed natural population analysis (NPA) charge based on natural bond orbital (NBO) computations[42] at the ωB97XD/def2-TZVP level for the oxygen atoms of **1** (−0.563), **2** (−0.645), and **3** (−0.450) become increasingly negative upon σ-hole bonding: **1a** (−0.600), **1b** (−0.603), **1c** (−0.612), and **1d** (−0.611) (see Fig. 1a), **2a** (−0.693), **2b** (−0.696), **2c** (−0.705), and **2d** (−0.702) (see Fig. 1b), **3a** (−0.477), **3b** (−0.478), **3c** (−0.482), and **3d** (−0.459) (see Fig. 1c).

Table 1 Computed σ-hole interaction energies, ΔE_{int} (kcal mol^{-1}), for **1(a–d)**, **2(a–d)** and **3(a–d)**, at MP2/def2-TZVP//ωB97XD/def2-TZVP

	ΔE_{int}		ΔE_{int}		ΔE_{int}
1a	−5.3	**2a**	−7.4	**3a**	−5.5
1b	−5.9	**2b**	−8.1	**3b**	−6.1
1c	−8.1	**2c**	−11.3	**3c**	−8.5
1d	−9.2	**2d**	−13.0	**3d**	−9.4

Direct comparisons of the ΔE_{int} values of **1(a–d)**, **2(a–d)**, and **3(a–d)** show a consistently lower σ-hole bonding interaction energy for the cyclopentadienone and cyclononatetraenone complexes, **1(a–d)** and **3(a–d)**, compared to the tropone complexes, **2(a–d)** (see Table 1). This can be explained by the effects of antiaromaticity gain in the five and nine membered ring, in **1(a–d)** and **3(a–d)**, (*i.e.*, increased cyclic [4*n*] π-electron delocalization) in contrast to aromaticity gain in the seven membered ring in **2(a–d)** (*i.e.*, increased cyclic [4*n* + 2] π-electron delocalization) (see Fig. 1). In concert, the C=O···X–R distances for **1(a–d)** and **3(a–d)** are shorter compared to those of **2(a–d)** (see Fig. 3).

Computed dissected $NICS(0)_{\pi zz}$ values[43,44] indicate that the four π-electron antiaromatic **1** ($NICS(0)_{\pi zz}$ = +19.4 ppm) becomes more antiaromatic upon tetrel ($\Delta NICS(0)_{\pi zz}$ = +3.3 ppm, **1a**), pnictogen ($\Delta NICS(0)_{\pi zz}$ = +3.8 ppm, **1b**), chalcogen ($\Delta NICS(0)_{\pi zz}$ = +4.4 ppm, **1c**), and halogen ($\Delta NICS(0)_{\pi zz}$ = +5.9 ppm, **1d**) bonding (see Table 2). In contrast, the formally six π-aromatic **2** ($NICS(0)_{\pi zz}$ = −6.7 ppm) becomes more aromatic upon tetrel ($\Delta NICS(0)_{\pi zz}$ = −3.2 ppm, **2a**), pnictogen ($\Delta NICS(0)_{\pi zz}$ = −3.7 ppm, **2b**), chalcogen ($\Delta NICS(0)_{\pi zz}$ = −4.4 ppm, **2c**), and halogen ($\Delta NICS(0)_{\pi zz}$ = −5.4 ppm, **2d**) bonding (see Table 2). Like **1(a–d)**, the planar eight π-electron antiaromatic **3** ($NICS(0)_{\pi zz}$ = +22.7 ppm) becomes more antiaromatic upon tetrel ($\Delta NICS(0)_{\pi zz}$ = +4.0 ppm, **3a**), pnictogen ($\Delta NICS(0)_{\pi zz}$ = +4.6 ppm, **3b**), chalcogen ($\Delta NICS(0)_{\pi zz}$ = +5.8 ppm, **3c**), and halogen ($\Delta NICS(0)_{\pi zz}$ = +8.0 ppm, **3d**) bonding (see Table 2). Negative $\Delta NICS(0)_{\pi zz}$ values indicate aromaticity gain upon σ-hole bonding. Positive $\Delta NICS(0)_{\pi zz}$ values indicate antiaromaticity gain upon σ-hole bonding. The tub-shaped cyclononatetraenone minimum shows little to no change in ring bond length upon σ-hole bonding (see geometries and discussion in the ESI†).

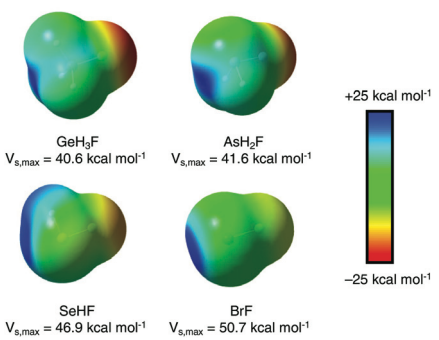

Fig. 2 Computed electrostatic potential maps for $GeHF_3$, AsH_2F, SeHF, and BrF based on a 0.001 au contour surface. Blue color indicates positive potential, red color indicates negative potential. $V_{S,max}$ shows the most positive electrostatic potential corresponding to the σ-hole.

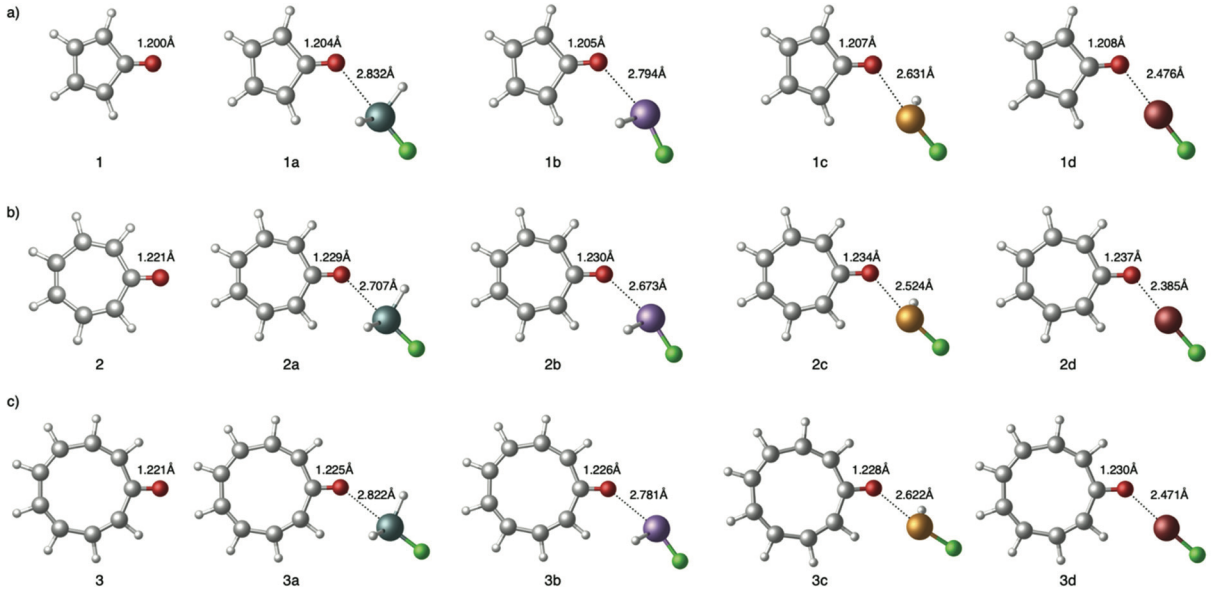

Fig. 3 Optimized geometries for (a) **1(a–d)**, (b) **2(a–d)**, and (c) **3(a–d)** at ωB97XD/def2-TZVP. Note more pronounced C═O bond lengthening in the σ-hole bonded tropone complexes **2(a–d)**.

Table 2 Computed $\Delta NICS(0)_{\pi zz}$ (in ppm) values for **1(a–d)**, **2(a–d)** and **3(a–d)**, computed $\Delta NICS(0)_{\pi zz}$ values are derived by comparing the computed $NICS(0)_{\pi zz}$ values for **1(a–d)**, **2(a–d)** and **3(a–d)**, to that of **1** ($NICS(0)_{\pi zz}$ = +19.4 ppm), **2** ($NICS(0)_{\pi zz}$ = −6.7 ppm), and **3** ($NICS(0)_{\pi zz}$ = +22.7 ppm) respectively. Positive $\Delta NICS(0)_{\pi zz}$ values indicate antiaromaticity gain, negative $\Delta NICS(0)_{\pi zz}$ values indicate aromaticity gain

	$\Delta NICS(0)_{\pi zz}$		$\Delta NICS(0)_{\pi zz}$		$\Delta NICS(0)_{\pi zz}$
1a	+3.3	**2a**	−3.2	**3a**	+4.0
1b	+3.8	**2b**	−3.7	**3b**	+4.6
1c	+4.4	**2c**	−4.4	**3c**	+5.8
1d	+5.9	**2d**	−5.4	**3d**	+8.0

Dissected $NICS(0)_{\pi zz}$[43,44] analyses were computed at PW91/def2-TZVP. $NICS(0)_{\pi zz}$ computations were performed by placing NICS points at the ring centers of **1–3** and extracting contributions only from the shielding tensor component perpendicular to the ring plane (*zz*) of all of the localized π-molecular orbitals (two C═C and one C═O π-bonds in **1**, three C═C and one C═O π-bonds in **2**, four C═C and one C═O π-bonds in **3**). $\Delta NICS(0)_{\pi zz}$ values were calculated by computed ring NICS $(0)_{\pi zz}$ values in the five, seven, and nine membered rings of the **1(a–d)**, **2(a–d)**, and **3(a–d)** complexes, minus the computed ring $NICS(0)_{\pi zz}$ values of the **1**, **2**, and **3** monomers.

π-Conjugated systems containing cyclopentadienone cores are useful organic electronics components, and the ability to modify their antiaromatic characters through σ-hole bonding interactions may have practical implications for their electronic properties.

9-Fluorenone, for example, contains a cyclopentadienone core fused to two benzenoid rings, and is extensively used as a precursor to synthesize a variety of organic electronics materials (see Fig. 4). Computed $NICS(0)_{\pi zz}$ values at the ring centers of the six (6MR) and five (5MR) membered rings of fluorenone (6MR: −23.1 ppm, −23.1 ppm, 5MR: +22.8 ppm) display increasing paratropicity as the C═O group engages in tetrel (6MR: −22.0 ppm, −22.7 ppm, 5MR: +24.3 ppm), pnictogen (6MR: −22.0 ppm, −22.6 ppm, 5MR: +24.3 ppm), chalcogen (6MR: −21.7 ppm, −22.1 ppm, 5MR: +24.9 ppm), and halogen (6MR: −20.7 ppm, −21.9 ppm, 5MR: +26.3 ppm) bonding. Following increased antiaromatic character in 9-fluorenone upon σ-hole bonding, the computed HOMO–LUMO gap for 9-fluorenone (3.61 eV) decreases when the exocyclic C═O bond forms tetrel (3.47 eV), pnictogen (3.46 eV), chalcogen (3.41 eV), and halogen (3.36 eV) bonding. Accordingly, the LUMO energy level for 9-fluorenone (−4.82 eV) lowers upon tetrel (−5.21 eV), pnictogen (−5.21 eV), chalcogen (−5.28 eV), and halogen (−5.39 eV) bonding. When two BrF groups form halogen bonding interactions to the carbonyl site of 9-fluorenone, the π-conjugated core shows even more pronounced paratropicity (6MR: −19.9 ppm, −19.9 ppm, 5MR: +28.2 ppm), the HOMO–LUMO gaps become narrower (3.21 eV), and the LUMO energy levels lower even more (−5.71 eV).

σ-Hole bonding interactions are finding an increasing number of applications in many areas of organic chemistry, *e.g.*, protein–ligand interactions, foldamer design, anion-

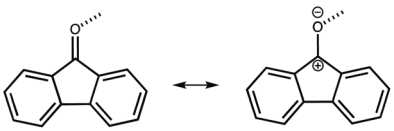

Fig. 4 Effects of σ-hole bonding on the resonance form of fluorenone.

sensing, and crystal engineering. Here, we highlight the effects of σ-hole bonding interactions on tuning (anti)aromaticity in ketocyclopolyenes, and their immediate consequence for tuning the electronic properties of fulvene-containing π-conjugated systems. Remarkably, σ-hole interactions are useful, not only for organizing the assembly of organic electronic components,[45] but also for tuning the electronic properties of extended π-conjugated systems, especially for those with formal [4*n*] antiaromatic character. We note also recent works discussing a relationship between the aromatic ring current of metalloporphyrins and the effects on halogen bonding interactions.[46]

Conflicts of interest

There are no conflicts to declare.

Acknowledgements

We thank the National Science Foundation (NSF) (CHE-1751370) and the National Institute of General Medical Sciences of the National Institute of Health (R35GM133548) for grant support.

Notes and references

1 J. I. Wu, J. E. Jackson and P. v. R. Schleyer, *J. Am. Chem. Soc.*, 2014, **136**, 13526–13529.
2 T. Kakeshpour, J. I. Wu and J. E. Jackson, *J. Am. Chem. Soc.*, 2016, **138**, 3427–3432.
3 P. Metrangolo, H. Neukirch, T. Pilati and G. Resnati, *Acc. Chem. Res.*, 2005, **38**, 386–395.
4 D. Mani and E. Arunan, *Phys. Chem. Chem. Phys.*, 2013, **15**, 14377–14383.
5 D. Mani and E. Arunan, *J. Phys. Chem. A*, 2014, **118**, 10081–10089.
6 S. J. Grabowski, *Phys. Chem. Chem. Phys.*, 2014, **16**, 1824–1834.
7 A. Bauzá, T. J. Mooibroek and A. Frontera, *Angew. Chem., Int. Ed.*, 2013, **52**, 12317–12321.
8 K. T. Mahmudov, A. V. Gurbanov, V. A. Aliyeva, G. Resnati and A. J. L. Pombeiro, *Coord. Chem. Rev.*, 2020, **418**, 213381.
9 S. Scheiner, *Acc. Chem. Res.*, 2013, **46**, 280–288.
10 L. Vogel, P. Wonner and S. M. Huber, *Angew. Chem., Int. Ed.*, 2019, **58**, 1880–1891.
11 J. Y. C. Lim and P. D. Beer, *Chemistry*, 2018, **4**, 731–783.
12 R. Gleiter, G. Haberhauer, D. B. Werz, F. Rominger and C. Bleiholder, *Chem. Rev.*, 2018, **118**, 2010–2041.
13 K. T. Mahmudov, M. N. Kopylovich, M. F. C. G. da Silva and A. J. L. Pombeiro, *Dalton Trans.*, 2017, **46**, 10121–10138.
14 G. Cavallo, P. Metrangolo, R. Milani, T. Pilati, A. Priimagi, G. Resnati and G. Terraneo, *Chem. Rev.*, 2016, **116**, 2478–2601.
15 D. Bulfield and S. M. Huber, *Chem. – Eur. J.*, 2016, **41**, 14434–14450.
16 P. Nagorny and Z. Sun, *Beilstein J. Org. Chem.*, 2016, **12**, 2834–2848.
17 R. Tepper and S. U. Schubert, *Angew. Chem., Int. Ed.*, 2018, **57**, 6004–6016.
18 J. S. Murray, P. Lane, P. Politzer and J. Leszczynski, *Int. J. Quantum Chem.*, 2007, **107**, 2286–2292.
19 J. S. Murray, P. Lane, T. Clark and P. Politzer, *J. Mol. Model.*, 2007, **13**, 1033–1038.
20 J. S. Murray, P. Lane and P. Politzer, *J. Mol. Model.*, 2009, **15**, 723–729.
21 P. Politzer, J. S. Murray and T. Clark, *Phys. Chem. Chem. Phys.*, 2010, **12**, 7748–7757.
22 P. Politzer, J. S. Murray and T. Clark, *Phys. Chem. Chem. Phys.*, 2013, **15**, 11178–11189.
23 T. Clark and A. Heßelmann, *Phys. Chem. Chem. Phys.*, 2018, **20**, 22849–22855.
24 K. E. Riley and P. Hobza, *J. Chem. Theory Comput.*, 2008, **4**, 232–242.
25 M. Palusiak, *J. Mol. Struct.: THEOCHEM*, 2010, **945**, 89–92.
26 S. M. Huber, E. Jimenez-Izal, J. M. Ugalde and I. Infante, *Chem. Commun.*, 2012, **48**, 7708–7710.
27 J. Thirman, E. Engelage, S. M. Huber and M. Head-Gordon, *Phys. Chem. Chem. Phys.*, 2018, **20**, 905–915.
28 S. J. Grabowski and W. A. Sokalski, *ChemPhysChem*, 2017, **18**, 1569–1577.
29 L. P. Wolters and F. M. Bickelhaupt, *ChemistryOpen*, 2012, **1**, 96–105.
30 S. H. Jungbauer, S. M. Walter, S. Schindler, L. Rout, F. Kneip and S. M. Huber, *Chem. Commun.*, 2014, **50**, 6281–6284.
31 A. Linke, S. H. Jungbauer, S. M. Huber and S. R. Waldvogel, *Chem. Commun.*, 2015, **51**, 2040–2043.
32 M. A. McAllister and T. T. Tidwell, *J. Am. Chem. Soc.*, 1992, **114**, 5362–5368.
33 K. Najafian, P. v. R. Schleyer and T. T. Tidwell, *Org. Biomol. Chem.*, 2003, **1**, 3410–3417.
34 T. Nozoe, *Non-Benzenoid Aromatic Compounds*, Interscience, New York, 1959, p. 339.
35 R. Pal, S. Mukherjee, S. Chandrasekhar and T. N. G. Row, *J. Phys. Chem. A*, 2014, **118**, 3479–3489.
36 M. J. S. Dewar, *Nature*, 1945, **155**, 50–51.
37 M. J. S. Dewar, *Nature*, 1950, **166**, 790–791.
38 T. Nozoe, S. Seto and T. Ikemi, *Proc. Jpn. Acad.*, 1951, **27**, 655–657.
39 M. J. Frisch, G. W. Trucks, H. B. Schlegel, G. E. Scuseria, M. A. Robb, J. R. Cheeseman, G. Scalmani, V. Barone, G. A. Petersson, H. Nakatsuji, X. Li, M. Caricato, A. V. Marenich, J. Bloino, B. G. Janesko, R. Gomperts, B. Mennucci, H. P. Hratchian, J. V. Ortiz, A. F. Izmaylov, J. L. Sonnenberg, D. Williams-Young, F. Ding, F. Lipparini, F. Egidi, J. Goings, B. Peng, A. Petrone, T. Henderson, D. Ranasinghe, V. G. Zakrzewski, J. Gao, N. Rega, G. Zheng,

W. Liang, M. Hada, M. Ehara, K. Toyota, R. Fukuda, J. Hasegawa, M. Ishida, T. Nakajima, Y. Honda, O. Kitao, H. Nakai, T. Vreven, K. Throssell, J. A. Montgomery Jr., J. E. Peralta, F. Ogliaro, M. J. Bearpark, J. J. Heyd, E. N. Brothers, K. N. Kudin, V. N. Staroverov, T. A. Keith, R. Kobayashi, J. Normand, K. Raghavachari, A. P. Rendell, J. C. Burant, S. S. Iyengar, J. Tomasi, M. Cossi, J. M. Millam, M. Klene, C. Adamo, R. Cammi, J. W. Ochterski, R. L. Martin, K. Morokuma, O. Farkas, J. B. Foresman and D. J. Fox, *Gaussian 16, Revision C.01*, Gaussian, Inc., Wallingford CT, 2016.

40 S. Kozuch and J. M. L. Martin, *J. Chem. Theory Comput.*, 2013, **9**, 1918–1931.

41 R. F. W. Bader, M. T. Carroll, J. R. Cheeseman and C. Chang, *J. Am. Chem. Soc.*, 1987, **109**, 7968–7979.

42 E. D. Glendening, C. R. Landis and F. Weinhold, *J. Comput. Chem.*, 2013, **34**, 1429–1437.

43 Z. Chen, C. S. Wannere, C. Corminboeuf, R. Puchta and P. v. R. Schleyer, *Chem. Rev.*, 2005, **105**, 3842–3888.

44 C. Corminboeuf, T. Heine, G. Seifert, P. v. R. Schleyer and J. Weber, *Phys. Chem. Chem. Phys.*, 2004, **6**, 273–276.

45 Z. R. Kehoe, G. R. Woller, E. D. Speetzen, J. B. Lawrence, E. Bosch and N. P. Bowling, *J. Org. Chem.*, 2018, **83**, 6142–6150.

46 J. Rani, V. Grover, S. Dhamija, H. M. Titi and R. Patra, *Phys. Chem. Chem. Phys.*, 2020, **22**, 11558–11566.